Insights on the thermal potential of a state-of-the-art palm oil/MXene nanofluid in a circular pipe

AS Abdelrazik [1*], Saidur R. [2, 3], FA Al-Sulaiman [1, 4]

[1] Interdisciplinary Research Center for Renewable Energy and Power Systems (IRC-REPS), King Fahd University of Petroleum & Minerals, Dhahran, Saudi Arabia

[2] Research Center for Nano-Materials and Energy Technology (RCNMET), School of Engineering and Technology, Sunway University, Bandar Sunway, Petaling Jaya, 47500, Selangor Darul Ehsan, Malaysia

[3] Department of Engineering, Lancaster University, Lancaster, LA1 4YW, UK

[4] Department of Mechanical Engineering, King Fahd University of Petroleum & Minerals, Dhahran, Saudi Arabia

*Corresponding Author: ahmeds@kfupm.edu.sa

Abstract

MXene, a recently created nanomaterial, offers significant potential for thermal, electrical, and a variety of other uses. MXene was utilized to generate heat transfer nanofluids with improved thermophysical properties for thermal applications and to establish the optimal parameters for achieving the best thermal performance. In this study, a palm oil/MXene nanofluid was used as the heat transfer fluid in a circular pipe to evaluate its thermal impact at different Reynolds numbers and applied heat fluxes at a range of introduced MXene nanoparticles' concentrations. Thermal conductivity and viscosity were shown to be linked to temperature and nanoparticle concentrations ranging from 0.01 to 0.1 mass%. The influence of concerted MXene nanoparticles (0.01 to 0.1 mass%) on the behavior of the PO/MXene nanofluid, was studied using CFD simulations at various flow Reynolds numbers (2,500 to 5,000) and wall heat fluxes (40,000 to 90,000 $W.m^{-2}$). The results indicate that increasing the nanoparticle concentration resulted in higher heat transfer coefficients and lower Nusselt numbers. MXene nanoparticles were more efficient at lowering the wall temperature and increasing the pace of cooling when applied at larger heat fluxes and lower Re numbers. The results reported in this article indicate that MXene nanomaterials have a strong potential for overcoming the low heat transfer difficulties encountered in heat exchange systems.

Keywords: MXene; Palm oil; Nanofluid; Thermal performance; Heat transfer; Thermal properties; CFD

1. Introduction

Enhancing the rate of heat transfer is one of the primary study areas in which researchers are interested [1]. Several techniques have been used to increase heat transfer, and several of these involve altering the design of a system by increasing the surface area [2] and incorporating fins. Additionally, the effect of the surrounding environment and ways to improve the properties of heat transfer fluids have been investigated. Numerous researchers have recently focused their attention on nanofluids as a novel and efficient heat

Nomenclature

T	temperature, ˚C	Δp	pressure drop, Pa/m
L	length of the pipe, m	h	heat transfer coefficient, $W.m^{-2}.K^{-1}$
D	pipe diameter, m	k	thermal conductivity, $W.m^{-1}.K^{-1}$
m	mass, kg	x	horizontal direction
Q	applied heat flux, W/m^2	y	vertical direction
c_p	specific heat, $J.kg^{-1}.K^{-1}$		
Greek symbols			
φ	nanoparticles mass concentration (mass%)	μ	dynamic viscosity, Pa.s
ρ	density, $kg\ m^{-3}$		
Subscripts			
nf	nanofluid	*np*	nanoparticles
bf	base fluid		
Abbreviations			
PO	Palm Oil	*Nu*	Nusselt Number
Re	Reynolds Number	*OPO*	Olein Palm Oil
EG	Ethylene Glycol	*GNP*	Graphene Nanoplatelets
SO	Soybean Oil	*POME*	Palm Oil Methyl Ester

transfer medium [3]. A nanofluid is a colloidal solution containing nanoparticles and a base fluid. Nanoparticles affect the thermophysical properties and flow characteristics of base fluids [4].

Nanofluids exhibit superior thermal characteristics to their base fluid and so have higher heat transfer coefficients, enhancing heat removal rates in heat exchange applications. Numerous nanofluids have been characterized to determine the extent to which their thermophysical properties have been enhanced and their impact on various heat transfer applications. Nanofluids have been used as heat exchange fluids in heat pipes due to their superior heat transfer enhancement [5–7].

Recent studies have demonstrated that MXene nanoparticles have the potential to significantly improve the heat transfer capability of a nanofluid prepared with them. Rubbi et al. [8] have conducted a numerical study, using COMSOL Physics, to study the optical and thermal properties and the dynamic and thermal stability of soybean oil/Mxene (SO/MXene). They employed a concentration range of 0.025 to 0.125 mass% of MXene and found that the suspension was stable up to 320 °C. At a concentration of 0.125 mass% and a temperature of 55 °C, dispersion of MXene increased thermal conductivity and specific heat by 60.82% and 24.49%, respectively, as compared to pure SO. At greater concentrations, increased viscosity and density were also noted. The performance of a hybrid photovoltaic/thermal (PV/T) system using SO/MXene as the heat exchange medium was demonstrated to be superior to that of standard heat transfer media such as water and alumina/water, as well as MXene/palm oil nanofluid. Additionally, the overall thermal efficiency of a system utilizing SO/MXene was 84.25%, while the electrical output was boosted by

15.44% when compared to a system utilizing water/alumina at 1000 $W.m^{-2}$. Similarly, Samylingam et al. [9] assessed the thermal and energy performance of an OPO/MXene nanofluid in a hybrid photovoltaic/thermal system. They examined performance in the range of 0.01 mass% to 0.2 mass% of MXene and discovered a 68.5% improvement in thermal conductivity at 0.2 mass% of MXene and 25 °C when compared to pure OPO. Additionally, the researchers discovered that when the temperature was increased from 25 to 50 °C, the viscosity of 0.2 mass% of MXene has reduced by up to 61%. OPO/MXene also has a higher thermal conductivity than water/Al_2O_3, with a 9% higher heat transfer coefficient.

In another study, Parashar et al. [10] evaluated the viscosity of a PO/MXene nanofluid containing less than 100 nm nanoparticles at concentrations ranging from 0.01 to 0.2 mass% and temperatures ranging from 18 to 100 °C. Their findings indicated that MXene had a greater effect at lower temperatures and that the viscosity increased with nanoparticle concentration. The authors created an empirical relationship to correlate the viscosity with the input temperature and concentration based on the results. The thermo-physical characteristics and stability of EG/MXene nanofluid have been studied by Bao et al. [4]. The researchers employed MXene nanosheets with a high aspect ratio, both as single-layer materials and as multilayer structures. Compared to pure EG, they found a 53.1% and a 64.9% increase in heat conductivity with 5 vol.% of multilayer and single-layer MXene, respectively. It was also shown that EG/MXene had a lower viscosity at 1 vol.% than MWCNT at 0.01 vol.%. For 30 days, no sedimentation was detected in the nanofluid based on single-layer MXene.

Using an IoNanofluid containing 0.2% of MXene at 30 °C, Parashar et al. [11] reported a maximum increase in thermal conductivity of roughly 48%. At 0.2 mass% and 23 °C, they found a maximum viscosity increase of 14.5% using MXene nanoparticles less than 100 nm. In a similar study using water/MXene nanofluid, Rafieerad et al. [12] observed an enhancement in thermal conductivity of 7.8 % and 17.9 % with 0.1% and 0.2% of MXene concentration in water/MXene nanofluid, respectively, as compared to non-covalent GNPs. Recently, Rahmadiawan et al. [13] examined the heat transfer effectiveness of the POME/MXene nanofluid. MXene with different concentrations in the range of 0.01 mass% to 0.1 mass% was introduced to synthesize five nanofluid samples. The authors reported more heat extraction at higher concentrations of the MXene nanoparticles as a result of increasing the thermal conductivity of the nanofluid sample, while no change was reported in the viscosity at different MXene concentrations.

Based on the investigations stated above and additional studies in the literature [13–17], the researchers have found that MXene nanoparticles can significantly improve the thermal characteristics and performance of nanofluids including them.

Although research has demonstrated the potential of palm oil (PO) as a heat transfer fluid and its ability to form nanofluids with nanoparticles (e.g. [18–20]), only a limited number of studies [10,21] have evaluated the thermal performance of the PO/MXene nanofluid. This work fills a gap in the scientific literature by describing the thermal behavior of the PO/MXene nanofluid at various Reynolds numbers and applied thermal loads. Determining the optimum working conditions for achieving the best thermal performance will provide a better understanding of the most appropriate heat transfer applications for the PO/MXene nanofluid. In addition, as the stability of nanofluids is one of the major challenges against the commercialization of several nanofluid types, different numerical approaches were implemented to indicate the expected performance of using a specific nanofluid in a specific application. Computational Fluid Dynamics (CFD) is considered one of the main tools used for this purpose with very good agreements with experimental data.

In this study, a two-dimensional steady-state CFD model has been developed to evaluate the thermal performance of the state-of-the-art PO/MXene nanofluid. The PO/MXene was used as a heat transfer fluid to extract heat from a circular-cross-section pipe with a constant applied heat flux to its wall. The performance of the nanofluid was evaluated under different applied dynamic and thermal conditions. The thermal performance of the nanofluid was assessed by evaluating the convection heat transfer coefficient, Nusselt number, and surface temperature, at different MXene nanoparticles' concentrations. The impact on the pressure drop across the pipe was also evaluated.

2. Methodology

In this section, the methodology used in the evaluation of the thermal performance of the PO/MXene nanofluid is described. A chart containing the steps followed to achieve this is shown in Figure 1. The chart illustrates the dependency of the present work on experimental measurements of the properties of the PO/MXene nanofluid, conducted through our group at an earlier time [9,13,22,23].

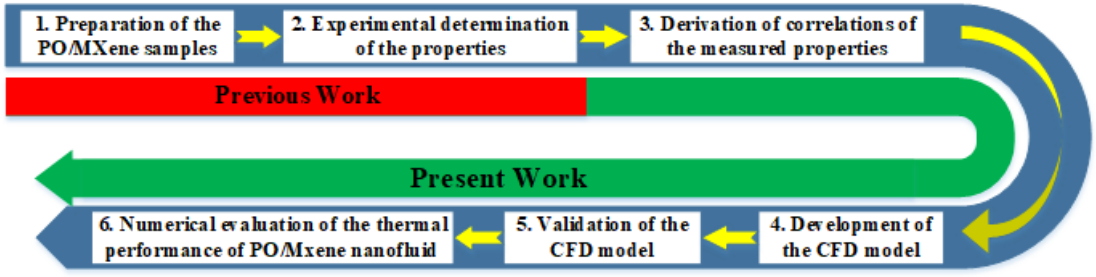

Figure 1. A chart of the steps of the assessment methodology.

2.1. Study configuration

The thermal performance of the PO/MXene nanofluid was evaluated using the nanofluid as the coolant of a circular-cross-sectional pipe. The main role of the PO/MXene nanofluid was to cool the surface of the wall of a pipe that was subjected to a constant heat flux. A schematic diagram of the tested circular pipe with its dimensions is illustrated in Figure 2. The dimensions of the pipe were selected to ensure the proper development of the fluid flow inside the pipe so that the nanofluid could be considered as fully developed during the performance evaluation.

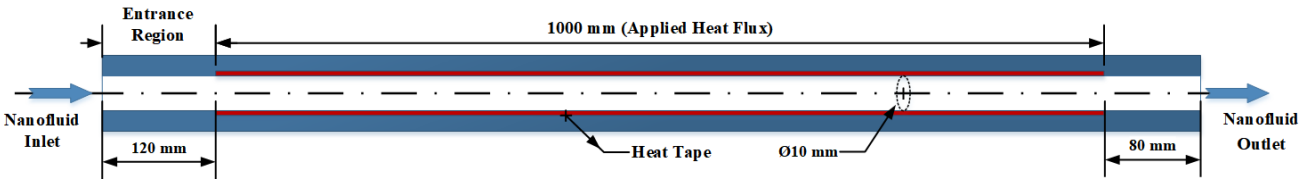

Figure 2. Schematic diagram of the evaluated pipe.

2.2. Development of the CFD model

ANSYS-Fluent 19 R3 was used to create a two-dimensional axisymmetric CFD model of the tested pipe with a circular-cross-section. Pressure-based and steady-state solutions were used. Solving for the fluid flow and heat transfer throughout the pipe, the energy, and the turbulent standard k-Ɛ models, with enhanced wall treatment, were implemented. The differential equations for continuity, momentum, and energy were solved to assess the overall thermal performance of the nanofluid in the pipe system under various thermal and dynamic boundary conditions applied to the moving PO/MXene nanofluid. To reduce the complexity of the current model, new simulation conditions were introduced as shown in Table 1. From these conditions is that the MXene/PO nanofluid is treated as a single-phase nanofluid with equivalent properties, evaluated using the correlations listed in Table 2, Table 3, Table 4, and Eq. 1. Single-phase approximation has been implemented in several research studies conducted to evaluate the thermal behavior of nanofluids. However, this approximation may cause a deviation or an overestimation of the evaluation parameters if these parameters are dependent on the optical properties of the nanofluid. Therefore, the presence of the two phases as well as the kind of the nanoparticles' distribution, in this case, is of high importance, as reported in [24,25].

A variety of cell counts were used to evaluate the model's mesh reliance, from 11,004 to 196,104.

Table 1. The introduced simulation conditions for the CFD model.

Serial #	Conditions
1	The piping wall is subjected to a constant heat flux.

2	The model is axisymmetric two-dimensional as the pipe has a circular cross-section.
3	The solution is time-independent (Steady-state condition).
4	The solution is based on pressure-based flow.
5	The circular pipe is simulated assuming a horizontal orientation (gravity has no effect).
6	The PO/MXene nanofluid is treated as a single-phase fluid with thermal conductivity and viscosity being the measured properties ([9,13,22,23], Table 2, and Table 3) and specific heat and density being the equivalent properties (Table 4 and Eq. 1).
7	The evaluated properties are temperature-dependent.

The governing mathematical relationships used for the evaluation of the equivalent properties and the assessment of the performance of the nanofluids under the aforementioned conditions in the form of differential equations are summarized in the following section.

2.3. Governing equations

2.3.1. Thermo-physical properties

The thermophysical properties of the PO/MXene nanofluid, for each single nanoparticles' concentration, have been introduced to the model in the form of temperature-dependent correlations. The correlations for the thermal conductivity and viscosity were developed using previously published experimental data through our group in [9,13,22,23] as shown in Table 2 and Table 3. On the other side, the specific heat correlations were derived from Maxwell relations by substituting the individual PO and MXene-specific heats at various temperatures as listed in Table 4. Considering the negligible changes in the density of the PO/MXene in the evaluated concentration range (0.01 mass% - 0.1 mass%) covered in the present study, a single correlation has been developed for the density of the samples considering the dependence of the PO density on the temperature as in Eq. 1.

Table 2. Correlation of the thermal conductivity of the PO/MXene nanofluid as a function of the temperature at different nanoparticle mass concentrations.

Conc. /mass%	Thermal conductivity*, k_{nf}/mW.m^{-1}.K^{-1}	$\bar{D}$/%
0	$k_{nf} = -1.273 \times 10^{-5} {T_{nf}}^4 + 2.883 \times 10^{-3} {T_{nf}}^3 - 0.2245 {T_{nf}}^2 + 7.233 T_{nf} + 84.9$	1.33
0.01	$k_{nf} = 2.929 \times 10^{-6} {T_{nf}}^5 - 7.993 \times 10^{-4} {T_{nf}}^4 + 0.08295 {T_{nf}}^3 - 4.058 {T_{nf}}^2 + 94.29 T_{nf} - 615$	0.23
0.03	$k_{nf} = 2.967 \times 10^{-6} {T_{nf}}^5 - 7.942 \times 10^{-4} {T_{nf}}^4 + 0.08082 {T_{nf}}^3 - 3.881 {T_{nf}}^2 + 88.94 T_{nf} - 535.6$	0.65
0.05	$k_{nf} = 3.933 \times 10^{-6} {T_{nf}}^5 - 1.062 \times 10^{-3} {T_{nf}}^4 + 0.1092 {T_{nf}}^3 - 5.309 {T_{nf}}^2 + 122.9 T_{nf} - 821.2$	0.86
0.08	$k_{nf} = 4.296 \times 10^{-6} {T_{nf}}^5 - 1.174 \times 10^{-3} {T_{nf}}^4 + 0.1214 {T_{nf}}^3 - 5.905 {T_{nf}}^2 + 136.8 T_{nf} - 874.9$	2.95
0.1	$k_{nf} = 3.15 \times 10^{-6} {T_{nf}}^5 - 8.394 \times 10^{-4} {T_{nf}}^4 + 0.08418 {T_{nf}}^3 - 3.934 {T_{nf}}^2 + 87.52 T_{nf} - 380.2$	0.45

*Where, k_{nf} in mW.m^{-1}.K^{-1} and T_{nf} in ˚C, and $\overline{D}$ is the average deviation of correlation from experimental data

Table 3. Correlations for the viscosity of the PO/MXene nanofluid as a function of the temperature at different nanoparticle mass concentrations.

Conc./mass%	Viscosity*, μ_{nf}/mPa.s	$\overline{D}$/%
0	$\mu_{nf} = -5.681 \times 10^{-7} {T_{nf}}^4 + 1.729 \times 10^{-4} {T_{nf}}^3 - 0.01885 {T_{nf}}^2 + 0.8259 T_{nf} - 8.516$	1.75
0.01	$\mu_{nf} = -5.226 \times 10^{-7} {T_{nf}}^4 + 1.567 \times 10^{-4} {T_{nf}}^3 - 0.01678 {T_{nf}}^2 + 0.7122 T_{nf} - 6.235$	0.43
0.03	$\mu_{nf} = -5.924 \times 10^{-7} {T_{nf}}^4 + 1.793 \times 10^{-4} {T_{nf}}^3 - 0.01945 {T_{nf}}^2 + 0.849 T_{nf} - 8.826$	1.14
0.05	$\mu_{nf} = -4.916 \times 10^{-7} {T_{nf}}^4 + 1.49 \times 10^{-4} {T_{nf}}^3 - 0.01613 {T_{nf}}^2 + 0.6927 T_{nf} - 6.222$	0.27
0.08	$\mu_{nf} = -4.923 \times 10^{-7} {T_{nf}}^4 + 1.477 \times 10^{-4} {T_{nf}}^3 - 0.01581 {T_{nf}}^2 + 0.6691 T_{nf} - 5.699$	0.36
0.1	$\mu_{nf} = -4.992 \times 10^{-7} {T_{nf}}^4 + 1.514 \times 10^{-4} {T_{nf}}^3 - 0.01642 {T_{nf}}^2 + 0.7072 T_{nf} - 6.478$	1.25

* Where, μ_{nf} is in mPa.s and T_{nf} is in ˚C

Table 4. Correlations of the specific heat of the PO/MXene nanofluid as a function of the temperature at different nanoparticle mass concentrations.

Conc./mass%	Specific heat*, $c_{p,nf}$/J.kg^{-1}.K^{-1}
0	$c_{p,nf} = 0.41 {T_{nf}}^2 - 66.84 T_{nf} + 4858.12$
0.01	$c_{p,nf} = 0.41 {T_{nf}}^2 - 66.83 T_{nf} + 4857.69$
0.03	$c_{p,nf} = 0.4 {T_{nf}}^2 - 66.82 T_{nf} + 4856.84$
0.05	$c_{p,nf} = 0.4 {T_{nf}}^2 - 66.8 T_{nf} + 4856$
0.08	$c_{p,nf} = 0.4 {T_{nf}}^2 - 66.78 T_{nf} + 4854.72$
0.1	$c_{p,nf} = 0.4 {T_{nf}}^2 - 66.77 T_{nf} + 4853.87$

* Where, $c_{p,nf}$ is in J.kg^{-1}.K^{-1} and T_{nf} is in ˚C.

$$\rho_f = 0.01 {T_f}^2 - 2.05 T_f + 946.769 \quad \textbf{Eq. 1}$$

Where, ρ_{nf} is in kg.m^{-3} and T_{nf} is in ˚C.

2.3.2. Mathematical differential equations

The continuity, momentum, and energy differential equations reported in [26,27] were used to model the present case as follows:

$$\frac{\partial u}{\partial x} + \frac{\partial v}{\partial y} = 0 \quad \textbf{Eq. 2}$$

where u and v are the components of the velocity of the nanofluid in the x and y directions.

The momentum equation:

$$\rho\left(u\frac{\partial u}{\partial x}+v\frac{\partial v}{\partial y}\right)=-\left(\frac{\partial p}{\partial x}+\frac{\partial p}{\partial y}\right)+\mu\left(\frac{\partial^2 u}{\partial x^2}+\frac{\partial^2 v}{\partial y^2}\right) \quad \textbf{Eq. 3}$$

where, ρ, p, and μ are the density, pressure, and dynamic viscosity of the PO/MXene nanofluid.

The energy equation:

$$\rho C_p\left(u\frac{\partial T}{\partial x}+v\frac{\partial T}{\partial y}\right)=-\frac{\partial(up)}{\partial x}-\frac{\partial(vp)}{\partial y}+k\left[\frac{\partial^2 T}{\partial x^2}+\frac{\partial^2 T}{\partial y^2}\right] \quad \textbf{Eq. 4}$$

where, C_p and k are the specific heat and thermal conductivity of the PO/MXene nanofluid.

2.3.3. Performance assessment equations

The performance of the PO/MXene nanofluid as a heat transfer fluid in a circular pipe was evaluated at different nanoparticle concentrations through the estimation of the heat transfer coefficient, Nusselt number, wall temperature, and pressure drop along the pipe. Similar parameters for the base PO fluid were also evaluated for comparison purposes. The heat transfer coefficient and Nusselt number were determined using Eq. 5 and Eq. 6 [26,27], respectively.

Heat transfer coefficient:

$$h=\frac{Nu\times k}{L} \quad \textbf{Eq. 5}$$

where Nu is the Nusselt number, k is the thermal conductivity of the fluid/nanofluid ($W.m^{-1}.K^{-1}$), and L is the length of the pipe (m).

Nusselt number:

$$Nu=\frac{Q\times D}{k(T_w-T_{av})} \quad \textbf{Eq. 6}$$

where Q is the constant heat flux (W), D is the pipe diameter (m), T_w is the wall temperature (K), and T_{av} is the average fluid temperature (K).

2.4. Validation of the CFD model

The model was validated against the experimentally-validated data of Abdelrazek et al. [28] to verify the accuracy of the developed CFD model for evaluating heat transfer in a pipe. Abdelrazek et al. [28] have evaluated the Nusselt number at different values of Reynold's number for deionized water (DW) flowing in a pipe. Constant heat flux was maintained at the surface of the pipe and the values of the other parameters used for the validation are summarized in Table 5. The results of the validation of the CFD model using the findings of Abdelrazek et al. [28] are described in the results and discussion section (3.2. Model validation).

Table 5. The parameters used for the validation of the CFD model using data published by Abdelrazek et al. [28].

Parameter	Value	Parameter	Value
The length of the pipe, *L*/m	1.2	Reynolds number, Re	6,000 – 11,000
The diameter of the pipe, *d*/cm	1	Inlet fluid temperature, T_{in}/°C	30
The applied heat flux, *Q*/W.m^{-2}	63,661.98	Moving fluid	Deionized water (DW)

2.5. Numerical evaluation of the performance

The validation of the CFD model was followed by the evaluation of the performance of the PO/MXene as a heat transfer fluid in the circular-cross-section pipe. The SIMPLE scheme was selected for the pressure-velocity coupling. The momentum and energy equations were solved using second-order upwind discretization, whereas the turbulent kinetic energy and dissipation rate equations were solved using first-order upwind discretization. The effect of the concentration of the MXene nanoparticles (φ) on the performance at different Reynolds numbers (Re) and applied heat fluxes (Q) was determined. First, the Reynolds number was varied in the range of 2,500 to 5,000 at a constant heat flux of 60,000 W.m^{-2}, followed by varying the heat flux in the range of 40,000 to 90,000 W.m^{-2} at a constant Reynolds number of 3,000. The heat transfer coefficient, Nusselt number, and wall temperature were used to compare the thermal performance using the PO/MXene nanofluid to the pure PO fluid. Besides, the pressure drop along the pipe was evaluated at the different Re numbers and MXene nanoparticles' concentrations. The Reynolds numbers employed in the study were chosen to ensure that performance is evaluated in turbulent operating circumstances. A summary of the studied and evaluated parameters is depicted in Figure 3.

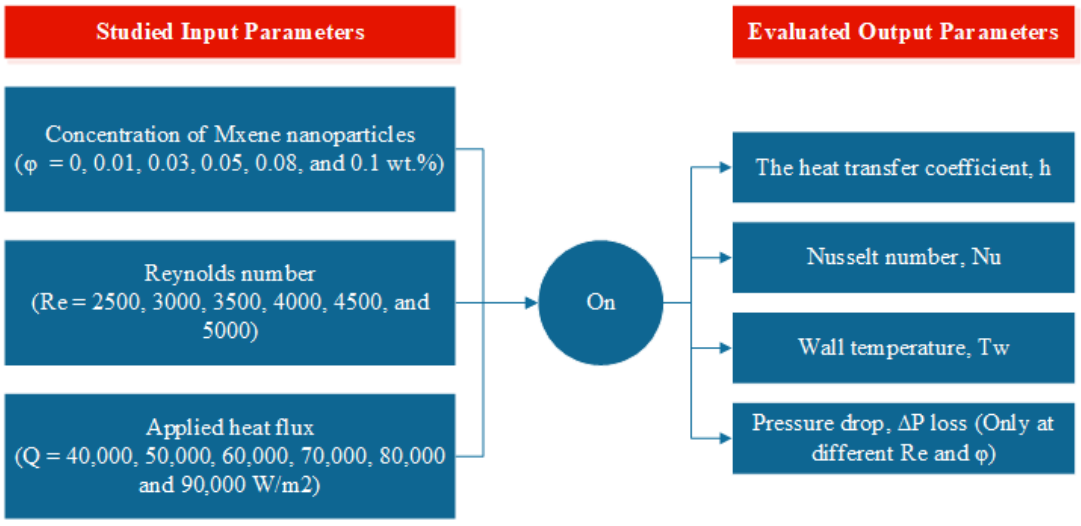

Figure 3. Studied and evaluated parameters used in the performance evaluation of the PO/MXene nanofluid.

3. Results and discussion

3.1. Grid independency test

As mentioned earlier, a grid independency test was conducted at several grid element numbers, i.e., 11,004, 24,000, 31,250, 74,998, and 196,104, to verify the reliability of the chosen grid size of the present study. The evaluation was based on the dependency level of the resulting wall temperature on the number of elements. Figure 4 shows the selected grid shape for the developed models with an employed boundary layer inflation near the wall. A very little variation in the temperature was observed starting from the number of elements of 24,000 as illustrated in Figure 5. The change in the wall temperature value between the model with 24,000 grids and the other one with 196,104 grids was less than 5.7%. Hence, and for safety, 31,250 was selected as the number of elements for the simulations conducted in the study, with a deviation of less than 3.7%.

3.2. Model validation

The results derived from the CFD model were compared with the results reported recently by Abdelrazek et al. [28] to validate the CFD model. Nusselt number was evaluated at different applied Reynolds numbers using the present model and under the same testing conditions listed in Table 5. Theresults were compared with those reported by Abdelrazek et al. [28]. The comparison shown in Figure 6 reveals that the results obtained using the CFD model agree well with the results reported by Abdelrazek et al. [28], with both sets of results following the same trend. The calculated difference between the two sets of results is less than 6% that can be attributed to the assumptions made and the few differences in the meshing scheme between the two studies.

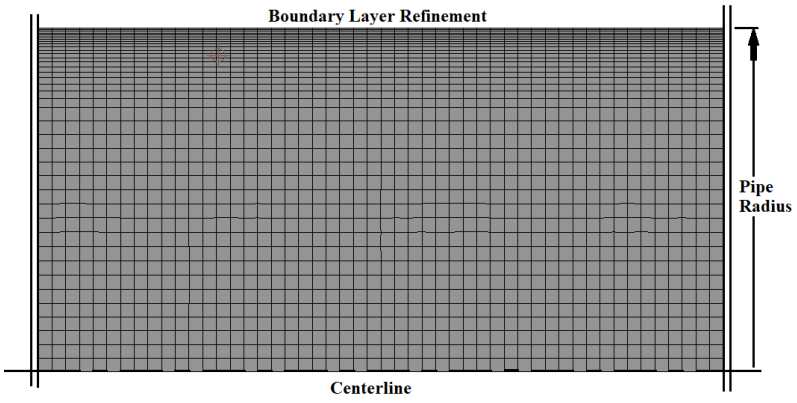

Figure 4. Selected grid shape for the developed models.

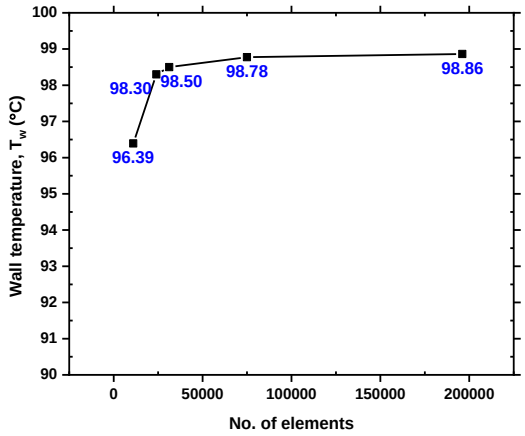

Figure 5. Variation of the wall temperature with the number of elements of the generated mesh.

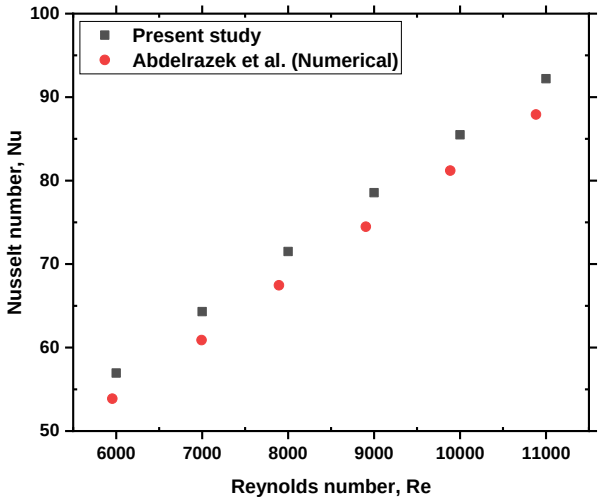

Figure 6. Comparison of the results obtained using the CFD model with the results presented by Abdelrazek et al. [28] **with DW as the fluid.**

3.3. Performance assessment

This section discusses the findings of the numerical evaluation of the impact of the Reynolds number (Re), of the fluid flow, and the applied heat flux (Q), to the pipe wall, on the performance of the PO/MXene nanofluid at different MXene nanoparticles' concentrations (φ). The performance was evaluated in terms of the heat transfer coefficient, Nusselt number (Nu), the wall temperature (T_w), and the pressure drop (ΔP_{loss}) along the pipe (at different Re numbers and φ).

3.3.1. Effect of the Reynolds number

Figure 7 shows the impact of the Reynolds number and the concentration of the nanoparticles on the heat transfer coefficient. The results in Figure 7 (a) indicate that better heat transfer coefficients could be obtained at higher Reynolds numbers. In comparison to the pure PO, increasing the Reynolds number from 2,500 to 5,000 results in an increase in the heat transfer coefficient by 63% and 68.1% at nanoparticles' concentrations of 0.01 mass% and 0.1 mass%, respectively. This was attributed to the higher convective heat transfer under high Re and flow velocities. Also, higher values of the heat transfer coefficient are achieved at higher nanoparticle concentrations as depicted in Figure 7(b), which agrees with the results reported in [13]. At a Re of 2500, adding 0.01 mass% and 0.1 mass% of MXene improves the heat transfer coefficient by 42.3% and 103.8%, respectively, compared to that of pure PO fluid. At a Re of 5,000, the equivalent percentage increase has decreased to 30.3% and 92.5%, respectively, which reveals a higher potential for thermal enhancement using the MXene nanoparticles, at lower Re values.

The effect of the Reynolds number on the Nusselt number is depicted in Figure 8. The results reveal that Nusselt numbers are higher at higher Reynolds numbers. However, the MXene concentration of more than 0.05 mass% negatively affects the Nusselt number. PO/MXene nanofluid with 0.01 mass% of nanoparticles possesses the highest Nusselt number (6.2% higher than PO at Re of 3,000), while PO/MXene with 0.1 mass% has the lowest Nu value (9.3% lower than PO at Re of 3,000). A noteworthy observation is the intermediate behavior of the PO base fluid. At a Re of 2500, Nu of the PO base fluid is comparable to the value for PO/MXene (0.05 mass%), while Nu starts to increase at a Re of 3,000, but remains lower than the values for the nanofluids with 0.01 mass% and 0.03 mass% of nanoparticles. At a Re of 3,500, the Nu of the PO base fluid becomes comparable to that for the 0.03 mass% nanofluid and continues to increase until the highest Nusselt number for the PO base fluid is reached at a Re of 5,000. The observed behavior is attributable to the combined effects of the heat transfer coefficient and the thermal conductivity of the fluid as both are affected by the MXene nanoparticles' concentration. As shown in Table 2, the change in thermal conductivity of the PO base fluid with temperature is negligible. In addition, the low improvement rates in the heat transfer coefficient that were reported earlier at a higher Reynolds number should result in a lowering of the Nusselt number of the PO/MXene nanofluid in comparison to that for the PO base fluid.

The temperature contours throughout the nanofluid boundary layer, taken in the mid of the pipe for selected values of Re numbers and MXene concentrations, are illustrated in Figure 9 and Figure 10, respectively. It can be declared that, at constant imposed heat flux, higher Re numbers, as well as higher MXene concentrations, resulting in more heat rejection from the pipe. It can be noticed that, at higher Re numbers, the impact of the MXene concentration on the reduction of temperatures becomes less effective. Replacing the base PO fluid with PO/MXene (0.1 mass%), the maximum temperature across the fluid has been

decreased by 30.1% at the Re number of 3,000, while the percentage becomes 23.6% at the Re number of 5,000, as depicted in Figure 7. It has to be mentioned that the aforementioned reduction percentages were evaluated using the maximum temperature values in °C.

Figure 11 shows how the concentration of the nanoparticles and Re influence the wall temperature of the circular pipe. The results indicate that the wall temperature decreases with the increasing concentration of the nanoparticles and Re. This behavior is opposite to that of the heat transfer coefficient, which decreases with increasing Re and concentration of the nanoparticles. For a given density and viscosity of nanofluids, the flow speed increases with increasing Re, values, which improves the heat transfer from the pipe wall resulting in lower wall temperatures. This is also due to better heat transfer owing to the higher thermal conductivities of the nanofluids at higher nanoparticle concentrations. At a Re of 2,500, the wall temperature decreases by 17.5% and 33.2% at an MXene concentration of 0.01 mass% and 0.1 mass%, respectively. At Re of 5,000, these percentages have decreased to 12.2% and 25.3%, respectively due to the lower percentages of heat transfer coefficient enhancements at higher Re as mentioned earlier. Figure 11 (b) shows that even a very small amount of 0.01 mass% of MXene is highly efficient in decreasing the wall temperature by 17.5% and 12.2% at Re values of 2,500 and 5,000, respectively. However, adding 0.02 mass%, to make the overall concentration 0.03 mass%, decreases the wall temperature only by another 5.1% and 4.3% at the same Re numbers.

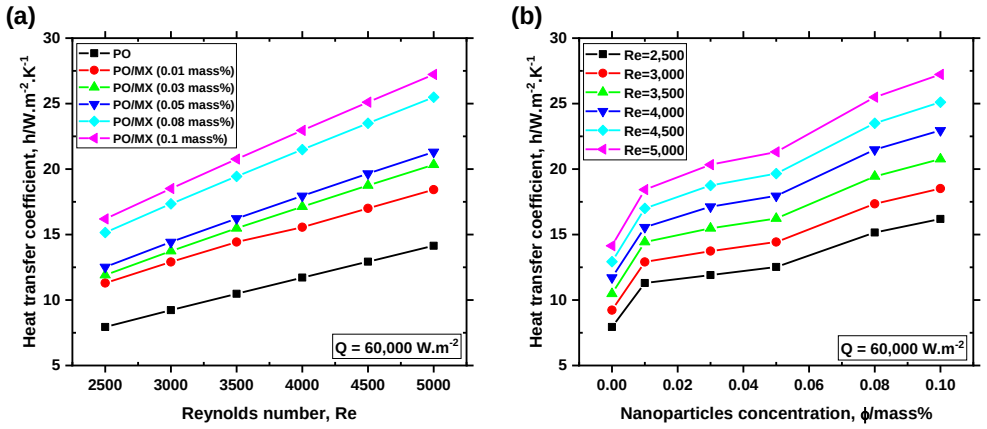

Figure 7. Effect of (a) the Reynold number and (b) the concentration of the nanoparticles on the heat transfer coefficient of the flowing nanofluid at a constant applied heat flux of 60,000 W.m^{-2}.

The increase of the pressure drop along the pipe with nanoparticles concentration was considered a drawback of the addition of nanomaterials to the conventional fluids. Therefore, the pressure drop along the pipe as a function of the concentration of the MXene nanoparticles at three selected Re values is depicted in Figure 12. Higher pressure drops are expected at higher Re numbers due to higher friction, low fluid

temperature, and higher viscosity. The relationship between the pressure drop and the concentration of the nanoparticles was also significant compared to the pressure drop for the PO base fluid. The increase in the pressure drop is 7.7% at an MXene concentration of 0.01 mass%. However, the increase in the pressure drop is not directly related to the increase in the concentration of the nanoparticles. For example, a ten-fold increase in the concentration of MXene (0.01 to 0.1 mass%) increases the pressure drop by only ~6.5%.

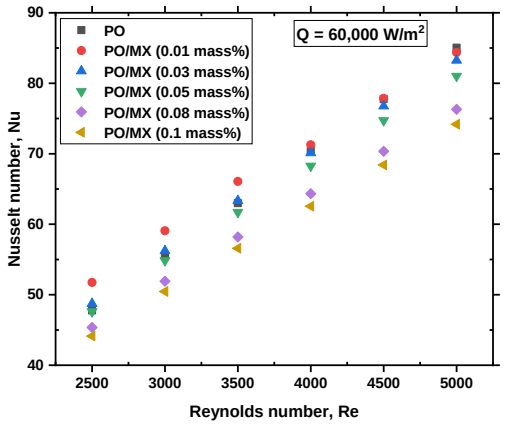

Figure 8. The dependence of the Nusselt number on the Reynolds number of the flowing nanofluid at different concentrations of the Mxene nanoparticles and a constant applied heat flux of 60,000 W.m^{-2}.

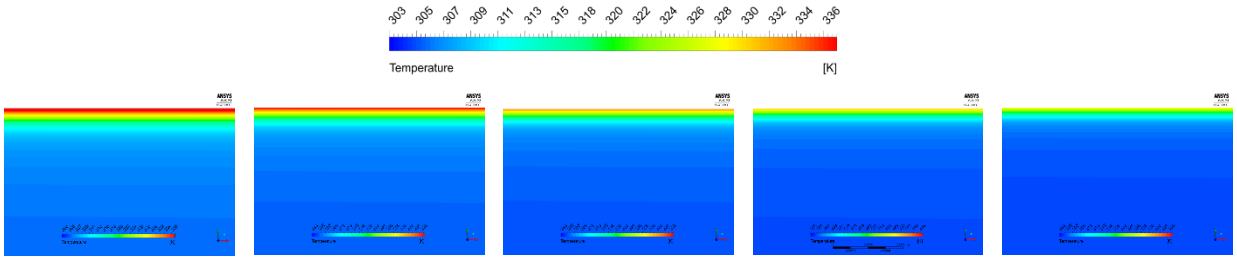

(a) Re=3,000 **(b) Re=3,500** **(c) Re=4,000** **(d) Re=4,500** **(e) Re=5,000**

Figure 9. Boundary layer temperature contours at different Re numbers, Q=60,000, and MXene concentration of 0.05 mass%. For comparison, the color map is similar for all contours and is defined using the profile at R=4,000.

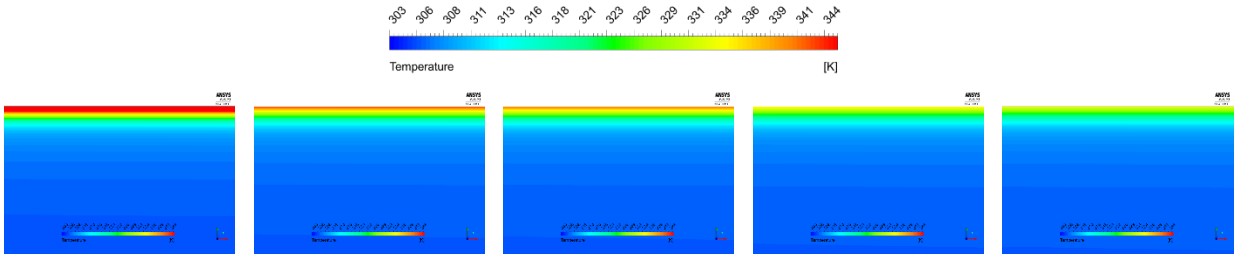

(a) φ=0 mass% **(b) φ=0.03 mass%** **(c) φ=0.05 mass%** **(d) φ=0.08 mass%** **(d) φ=0.1 mass%**

Figure 10. Boundary layer temperature contours at different MXene concentrations, Re=3,000, and Q=60,000. For comparison, the color map is similar for all contours and is defined using the profile at φ=0.05 mass%.

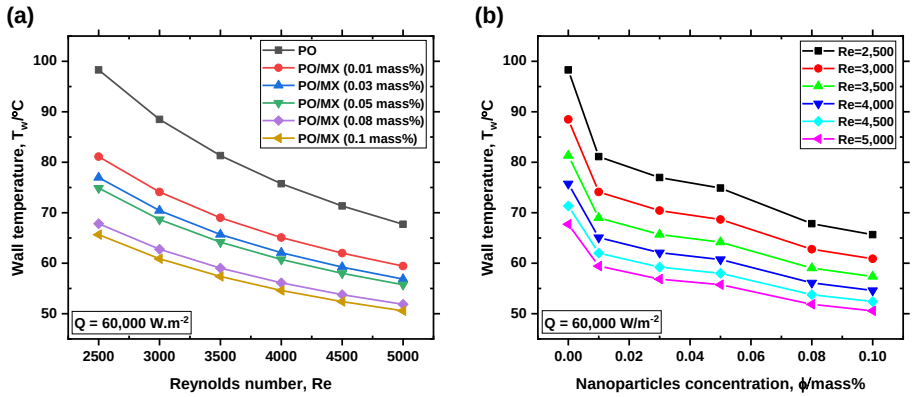

Figure 11. Effect of (a) the Reynold number and (b) the concentration of the nanoparticles of the flowing nanofluid on the wall temperature of the pipe at a constant applied heat flux of 60,000 W.m^{-2}.

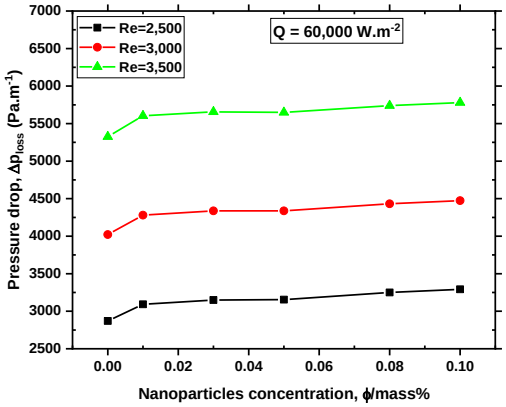

Figure 12. The dependence of the pressure drop along the nanofluid pipe on the concentration of the Mxene nanoparticles at different values of the Reynolds number and a constant applied heat flux of 60,000 W.m^{-2}.

3.3.2. Effect of the applied heat flux

The effects of the applied heat flux on the performance of the PO/MXene nanofluid are described in this section. Figure 13 shows the dependence of the heat transfer coefficient of the flowing PO/MXene nanofluid on the heat flux applied to the wall of the pipe, and the concentration of the nanoparticles at a constant Re of 3,000. The results depicted in Figure 13(a) show that the variation of the heat transfer

coefficient with the applied heat flux is almost negligible at a given concentration of the fluid/nanofluid, which is considered as due to the constant applied Re number. The results in Figure 13(b) do confirm that the applied heat flux does not significantly affect the heat transfer coefficient at a given concentration of the nanoparticles and a Re of 3,000. However, the heat transfer coefficient significantly increases with the concentration of the nanoparticles. The results in Figure 13(b) reveal that for a MXene concentration of 0.01 mass%,the heat transfer coefficient is improved by 30.9% at an applied heat flux of 40,000 $W.m^{-2}$, while the improvement exceeds 90% at 0.1 mass%.

Variation of the Nusselt number with the applied heat flux and the concentration of the nanoparticles is depicted in Figure 14. At a given concentration, the variation in the Nusselt number with the applied heat flux is considered small (Figure 14(a)). The largest calculated variation is less than 3% when the applied heat flux is varied from 40,000 to 90,000 $W.m^{-2}$, which is negligible. However, the Nusselt number is highly dependent on the concentration of the nanoparticles. The Nusselt number is higher at lower nanoparticle concentrations, which is attributed, as explained earlier, to the differences in the variation of the heat transfer coefficient and the thermal conductivity when the concentration is varied. For instance, when the concentration is increased from 0.01 mass% to 0.03 mass% the thermal conductivity increases by 12.3% on average in the temperature range of 25-85 °C, while the increase in the heat transfer coefficient is 9.77% on average in the same temperature range. The increase of the thermal conductivity with the increase of the concentration of nanoparticles is much higher than the increase of the heat transfer coefficient for a similar increase of concentration, resulting in the decrease of the Nusselt number with the increasing concentration of the MXene nanoparticles. Similarly, as described in the previous section, the behavior observed is different when compared to the base PO fluid. However, in general, the Nusselt number of PO/MXene nanofluids is higher than that of the base PO fluid, as shown in Figure 14(b). On the other side, an opposite trend is observed for the change of the Nu values for the PO with the applied heat fluxes. It is observed that Nu decreased with the increase in the applied heat flux values. This is attributed to the fact that increasing the heat flux causes an increase in the temperature of the PO fluid, which results in higher PO thermal conductivity, with almost no changes in the heat transfer coefficient that results in lowering the Nu values.

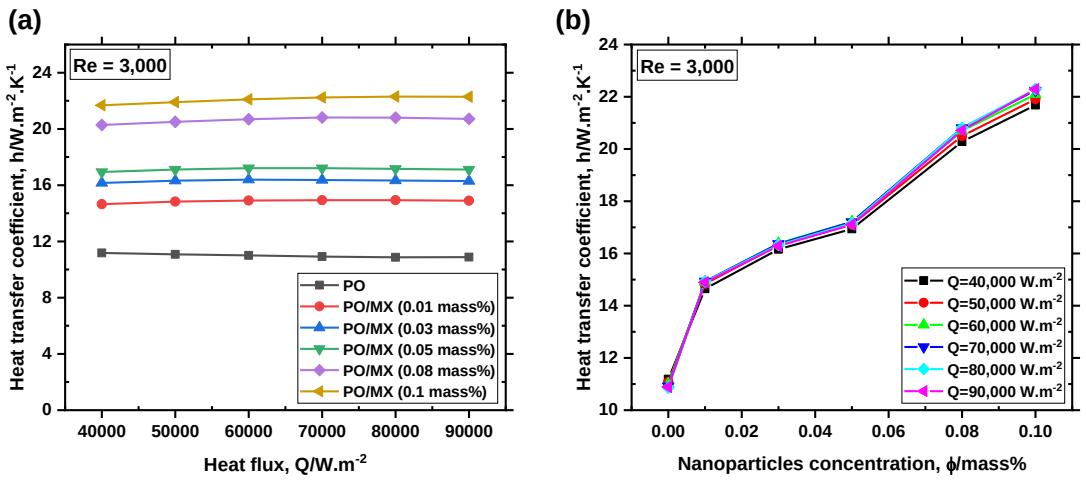

Figure 13. Effect of (a) the heat flux applied to the wall of the pipe and (b) the concentration of the nanoparticles on the heat transfer coefficient of the flowing nanofluid at a Reynolds number of 3,000.

The temperature contours throughout the nanofluid boundary layer for selected values of the wall heat flux, taken in the mid of the pipe and at an MXene concentration of 0.05 mass%, are illustrated in Figure 15. Higher temperature levels are noticed at higher values of the applied heat flux to the piping wall.

Figure 16 shows the variation of the wall temperature with the applied heat flux and the concentration of the nanoparticles at a constant Reynolds number. The highest wall temperature is observed for the highest applied heat flux when the base PO fluid is used (Figure 16 (a)). Increasing the applied heat flux increases the temperature of the wall. In addition, the inclusion of MXene nanoparticles in PO is highly efficient in decreasing the wall temperature. Moreover, the rate of increase in temperature is lower with increasing applied heat flux at higher concentrations of nanoparticles. The results depicted in Figure 16 (a) show that the wall temperature increases by 61.3% and 49.7% for nanofluids with 0.01 mass% and 0.1 mass% MXene, respectively when the applied heat flux is increased from 40,000 to 90,000 $W.m^{-2}$. The highest increase in the wall temperature of 74.1% is for pure PO.

It is declared that, at a constant Re number, higher MXene concentrations are more efficient at higher heat fluxes allowing for more heat rejection from the pipe. Replacing the base PO fluid with PO/MXene (0.1 mass%), the maximum temperature across the fluid has been decreased by 28.4% for an applied heat flux of 50,000 $W.m^{-2}$, while it was decreased by 34.2% for an applied heat flux of 90,000 $W.m^{-2}$. The results in Figure 16 (b) show that the effect of adding nanoparticles is more pronounced at higher applied fluxes. Adding only 0.01 mass% of MXene decreases the wall temperature by 12.5% at an applied heat flux of 40,000 W/m^2. The decrease in wall temperature increases to 18.9% at an applied heat flux of 90,000 $W.m^{-2}$. Again, the aforementioned percentages were evaluated using the maximum temperature values in °C.

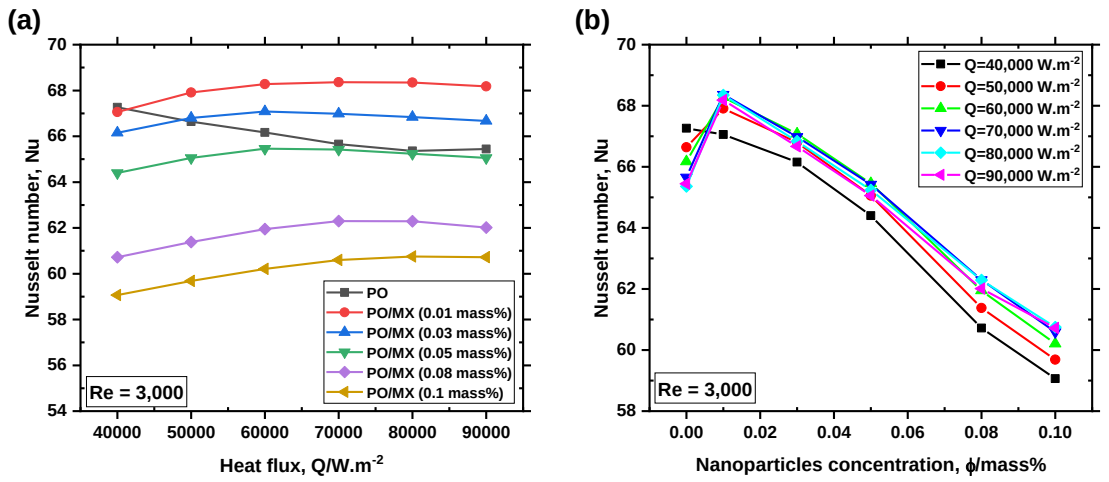

Figure 14. Effect of (a) the heat flux applied to the wall of the pipe and (b) the concentration of the nanoparticles on the Nusselt number of the flowing nanofluid at a constant Reynolds number of 3,000.

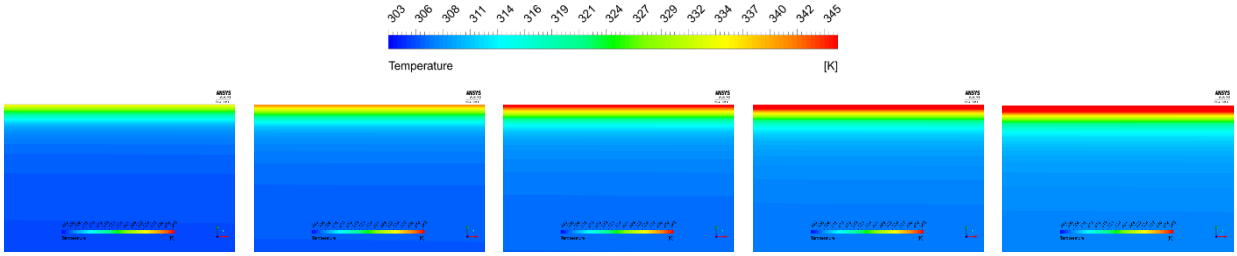

(a) Q=50,000 W.m^{-2} **(b) Q=60,000 W.m^{-2}** **(c) Q=70,000 W.m^{-2}** **(d) Q=80,000 W.m^{-2}** **(e) Q=90,000 W.m^{-2}**

Figure 15. Boundary layer temperature contours at different heat fluxes, Re=3,000, and MXene concentration of 0.05 mass%. For comparison, the color map is similar for all contours and is defined using the profile at Q=60,000 W.m^{-2}.

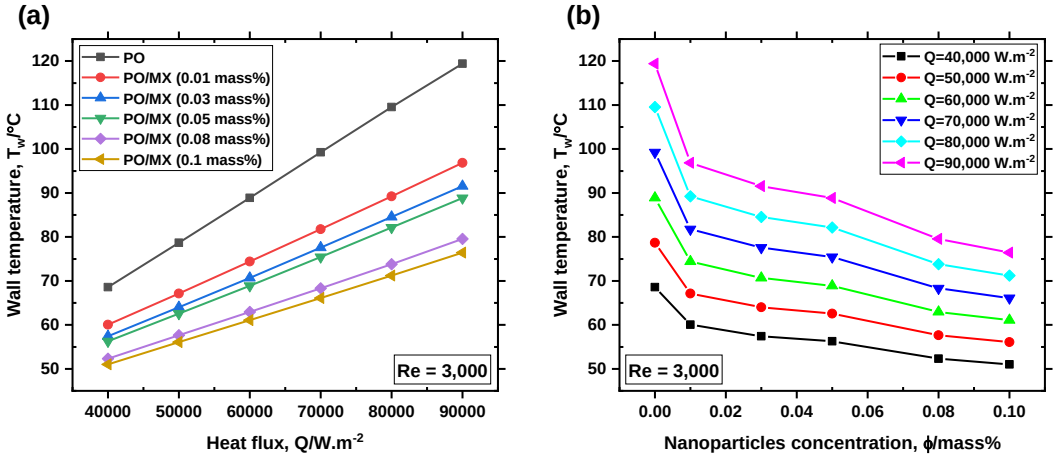

Figure 16. Effect of (a) the heat flux applied to the wall of the pipe and (b) the concentration of the nanoparticles on the wall temperature of the nanofluid pipe at a constant Reynolds number of 3,000.

4. Conclusions

In this article, the effect of the concertation of MXene nanoparticles on the performance of the PO/MXene nanofluid under various thermally and dynamically applied conditions is discussed. A Computational Fluid Dynamics (CFD) 2D and steady-state model was developed and validated to evaluate the performance of the PO/MXene nanofluid used as a coolant fluid flowing through a circular cross-sectional pipe. The evaluation was conducted at different Reynolds numbers and applied heat fluxes. The analysis of the results leads to the following main conclusions:

- MXene nanomaterial is proven as a highly efficient nanomaterial for boosting the thermal performance of a base fluid prepared with them.
- Higher thermal conductivities and convective heat transfer coefficients are achieved at higher concentrations of the MXene nanoparticles.
- The different rates of improvement between the thermal conductivity and heat transfer coefficient results in lowering the Nusselt number of the PO/MXene nanofluids at higher concentrations.
- The rate of increase in the thermal conductivity with the increase of the concentration is higher than that for the heat transfer coefficient.
- Increasing the Reynolds number positively influences the heat transfer coefficient and lowers the wall temperature, whilethe impact of the concentration of MXene nanoparticles, in boosting the heat rejection, is more pronounced at lower Re numbers.
- Higher pressure drops are achieved at higher Reynolds numbers, while the effect of the concentration of the nanoparticles is insignificant.
- The effect of variation of the applied heat flux, at constant Re and MXene concentration, on the heat transfer coefficient is almost negligible.
- MXene nanoparticles are more efficient in decreasing the wall temperature and increasing the rate of the wall temperature reduction at higher heat fluxes.
- The largest improvement in the thermal performance, in comparison to the base PO, is observed for the PO/MXene nanofluid with the lowest concentration (0.01 mass%), while the improvement is lower for further increases in the concentration of the MXene nanoparticles.

The conclusions reveal that MXene nanomaterial has a high potential as an excellent solution to overcome the low heat transfer problems in heat exchange systems. Further studies should be conducted to evaluate the performance of different MXene-based nanofluids and improve their stability, which is a major shortcoming preventing their application.

5. References

1. Mahian O, Kolsi L, Amani M, Estellé P, Ahmadi G, Kleinstreuer C, et al. Recent advances in modeling and simulation of nanofluid flows — Part I : Fundamentals and theory. Phys Rep [Internet]. Elsevier B.V.; 2019;790:1–48. Available from: https://doi.org/10.1016/j.physrep.2018.11.004

2. Wen D, Lin G, Vafaei S, Zhang K. Review of nanofluids for heat transfer applications. Particuology. 2009;7(2):141–50.

3. Sajid MU, Ali HM. Recent advances in application of nanofluids in heat transfer devices : A critical review. Renew Sustain Energy Rev [Internet]. Elsevier Ltd; 2019;103:556–92. Available from: https://doi.org/10.1016/j.rser.2018.12.057

4. Bao Z, Bing N, Zhu X, Xie H, Yu W. Ti3C2Tx MXene contained nanofluids with high thermal conductivity, super colloidal stability and low viscosity. Chem Eng J [Internet]. Elsevier; 2021;406:126390. Available from: https://doi.org/10.1016/j.cej.2020.126390

5. Nazari MA, Ahmadi MH, Sadeghzadeh M, Shafii MB, Goodarzi M. A review on application of nanofluid in various types of heat pipes. J Central South Univ. 2019;26(5):1021–41.

6. Poplaski LM, Benn SP, Faghri A. Thermal performance of heat pipes using nanofluids. Int J Heat Mass Transf. 2017;107:358–71.

7. Sureshkumar R, Mohideen ST, Nethaji N. Heat transfer character- istics of nanofluids in heat pipes: a review. Renew Sustain Energy Rev. 2013;20:397–410.

8. Rubbi F, Habib K, Saidur R, Aslfattahi N, Yahya SM, Das L. Performance optimization of a hybrid PV/T solar system using Soybean oil/MXene nanofluids as A new class of heat transfer fluids. Sol Energy [Internet]. Elsevier; 2020;208:124–38. Available from: https://doi.org/10.1016/j.solener.2020.07.060

9. Samylingam L, Aslfattahi N, Saidur R, Mohd S, Afzal A. Thermal and energy performance improvement of hybrid PV/T system by using olein palm oil with MXene as a new class of heat transfer fluid. Sol Energy Mater Sol Cells [Internet]. Elsevier B.V.; 2020;218:110754. Available from: https://doi.org/10.1016/j.solmat.2020.110754

10. Parashar, N., Aslfattahi, N., Yahya, S.M. and Saidur, R., 2021. An artificial neural network approach for the prediction of dynamic viscosity of MXene-palm oil nanofluid using experimental data. Journal of Thermal Analysis and Calorimetry, 144(4), pp.1175. 2020.

11. Parashar N, Aslfattahi N, Yahya SM, Saidur R. ANN Modeling of Thermal Conductivity and Viscosity of MXene-Based Aqueous IoNanofluid. Int J Thermophys [Internet]. Springer US; 2021;42:1–24.

Available from: https://doi.org/10.1007/s10765-020-02779-5

12. Rafieerad, M., et al. New water-based fluorescent nanofluid containing 2D titanium carbide MXene sheets: a comparative study of its thermophysical, electrical and optical properties with amine and carboxyl covalently functionalized graphene nanoplatelets.

13. Rahmadiawan D, Aslfattahi N, Nasruddin N, Saidur R. Rahmadiawan, D., Aslfattahi, N., Nasruddin, N., Saidur, R., Arifutzzaman, A. and Mohammed, H.A., 2021. MXene based palm oil methyl ester as an effective heat transfer fluid. In Journal of Nano Research (Vol. 68, pp. 17-34). Trans Tech Publications Ltd. 2021;

14. Aslfattahi N, Samylingam L, Abdelrazik AS, Arifutzzaman A, Saidur R. MXene based new class of silicone oil nanofluids for the performance improvement of concentrated photovoltaic thermal collector. Sol Energy Mater Sol Cells [Internet]. Elsevier B.V.; 2020;211:110526. Available from: https://doi.org/10.1016/j.solmat.2020.110526

15. Aslfattahi, Navid, et al. Experimental investigation of energy storage properties and thermal conductivity of a novel organic phase change material/MXene as A new class of nanocomposites. Journal of Energy Storage 27 2020; 101115.

16. Das L, Habib K, Saidur R, Aslfattahi N, Yahya SM, Rubbi F. Improved thermophysical properties and energy efficiency of aqueous ionic liquid/mxene nanofluid in a hybrid pv/t solar system. Nanomaterials. 2020;10:1–26.

17. Bakthavatchalam B, Habib K, Saidur R, Aslfattahi N, Yahya SM, Rashedi A, et al. Optimization of thermophysical and rheological properties of mxene ionanofluids for hybrid solar photovoltaic/thermal systems. Nanomaterials. 2021;

18. Javed M, Shaik AH, Khan TA, Imran M, Aziz A, Ansari AR, et al. Synthesis of stable waste palm oil based CuO nanofluid for heat transfer applications. Heat Mass Transf und Stoffuebertragung. Heat and Mass Transfer; 2018;54:3739–45.

19. Hussein AM, Lingenthiran, Kadirgamma K, Noor MM, Aik LK. Palm oil based nanofluids for enhancing heat transfer and rheological properties. Heat Mass Transf und Stoffuebertragung. Heat and Mass Transfer; 2018;54:3163–9.

20. Ramachandran S, Kalaichelvi P, Sundaram S. Heat transfer studies in a spiral plate heat exchanger for water - palm oil two phase system. Brazilian J Chem Eng. 2008;25:483–90.

21. Samylingam L, Aslfattahi N, Saidur R, Yahya SM, Afzal A, Arifutzzaman A, et al. Thermal and energy

performance improvement of hybrid PV/T system by using olein palm oil with MXene as a new class of heat transfer fluid. Sol Energy Mater Sol Cells [Internet]. Elsevier B.V.; 2020;218:110754. Available from: https://doi.org/10.1016/j.solmat.2020.110754

22. Khan J, Aslfattahi N, Yahya SM. Prediction of the dynamic viscosity of MXene / palm oil nanofluid using support vector regression. 2021;

23. Parashar N, Aslfattahi N, Mohd S, Saidur YR. An artificial neural network approach for the prediction of dynamic viscosity of MXene - palm oil nanofluid using experimental data. J Therm Anal Calorim [Internet]. Springer International Publishing; 2021;144:1175–86. Available from: https://doi.org/10.1007/s10973-020-09638-3

24. Bårdsgård R, Kuzmenkov DM, Kosinski P, Balakin B V. Eulerian CFD model of direct absorption solar collector with nanofluid. J Renew Sustain Energy. AIP Publishing LLC; 2020;12.

25. Sharaf OZ, Al-khateeb AN, Kyritsis DC, Abu-nada E. Direct absorption solar collector (DASC) modeling and simulation using a novel Eulerian-Lagrangian hybrid approach : Optical , thermal , and hydrodynamic interactions. Appl Energy [Internet]. Elsevier; 2018;231:1132–45. Available from: https://doi.org/10.1016/j.apenergy.2018.09.191

26. Cengel YA. Ghajar. Heat and Mass Transfer-Fundamentals and applications. Mc Graw Hill, fourth edition. 2011.

27. Incropera, Frank P., David P. DeWitt, Theodore L. Bergman, and Adrienne S. Lavine. Fundamentals of heat and mass transfer. Vol. 6. New York: Wiley, 1996.

28. Abdelrazek AH, Kazi SN, Alawi OA, Yusoff N, Oon CS, Ali HM. Heat transfer and pressure drop investigation through pipe with different shapes using different types of nanofluids. J Therm Anal Calorim [Internet]. Springer International Publishing; 2020;139:1637–53. Available from: https://doi.org/10.1007/s10973-019-08562-5